Talanta 201 (2019) 96–103

Contents lists available at ScienceDirect

Talanta

journal homepage: www.elsevier.com/locate/talanta

Fluorescence nano metal organic frameworks modulated by encapsulation for construction of versatile biosensor

Shuguang Yan[a], Dongyan Deng[b], Lichun Zhang[b], Yi Lv[a,b,*]

[a] Analytical & Testing Center, Sichuan University, Chengdu, Sichuan, 610064, China
[b] Key Laboratory of Green Chemistry & Technology, Ministry of Education, College of Chemistry, Sichuan University, Chengdu, Sichuan, 610064, China

ARTICLE INFO

Keywords:
Encapsulation
Thrombin
Au nanoclusters
MOFs nanocomposites
Fluorescence biosensors

ABSTRACT

The versatile fluorescence biosensors were implemented based on multipurpose nano metal organic frameworks (nMOFs) nanocomposites, which were obtained as fluorescence signal probes through encapsulation nMOFs. In this modulation process, the encapsulant bind with nMOFs through electrostatic attraction and hydrogen bond. Meanwhile, fluorescence enhancement of nMOFs were observed, accompanied by an increased in water solubility. The specific combination of target analyte triggers the release of the encapsulant and allows the target analyte to bind encapsulant to form a stable analyte-encapsulant complex. The complex binds tightly and promotes the photoinduced electron transfer from MOFs nanocomposites to the complex, thus resulting in reduce the fluorescence intensity of the MOFs nanocomposites. The results indicated that this novel system enables the specific and versatile detection of target biomolecules such as hemin and folic acid with high sensitivity and selectivity based on the choices of different encapsulant. Under optimized conditions, these biosensors show high sensitivity with a linear range from 0.16 to 12.5 μg/mL for hemin and 0.15–17.5 μmol/L for folic acid and detection limit of 47 ng/mL for hemin and 45 nmol/L folic acid. Moreover, it exhibits good performance of excellent selectivity, high stability, and acceptable fabrication reproducibility. This new multipurpose MOFs nanocomposites open avenues for combining together their properties and functionalities, and displaying novel important applications in fluorescence biosensors.

1. Introduction

MOFs greatly expand the applications in many fields such as bioanalysis, biocatalysis, and biomedical engineering [1–5]. Remarkably, fluorescence MOFs have blossomed out as advantageous chemical biosensors because of their easily introduced photoluminescence, various properties in structural, permanent porosity, functional recognition sites and numerous response mechanisms, meanwhile, regulable functionality stick out compare to other traditional fluorescence sensors [6–8]. It has been reported that MOFs have been satisfactorily used as effective fluorescence probe for bioactive molecule [9–11]. These suggested that MOFs have advantages of extending applications of the functionalized MOFs in the field of biosensors [12,13].

Among the fluorescence MOFs, nMOFs are preeminent candidates to be applied to photoluminescence devices because of their structural diversity and adjustable emission [14–16]. It demonstrated that fluorescence water solubility nMOFs may exhibit various and excellent optical properties. Therefore, optimized nMOFs can promisingly represent the new generation of fluorescence materials with a profound impact [17]. However, following with the size of MOFs reducing to nanoscale, the metal ions and organic ligands of nMOFs surface will not be totally coordinated and lead to the nMOFs carry different charges [18], and the fluorescence property of nMOFs need to be further improved. Fluorescence can be fine-regulated by kinds of strategies within MOFs. Firstly, the spectra of MOFs can be accurately adjusted by the number of captured fluorophores [19]. The other is the emission spectra can be adjusted by using the commixture of lanthanide ions in diverse ratios [20]. The most importantly, the efficient passivation for the surface of nMOFs by encapsulating on the host allows for an increment of the fluorescence properties [21,22]. In recent years, multipurpose encapsulated nMOFs have been obtained more and more attention. Kinds of multipurpose encapsulated nMOFs have been prepared through the introduction of functional molecules [23–25]. The mild obtaining conditions of surface adsorption make it ideal for the preservation and activation of structure [26–28]. Therefore, the fluorescence regulation and encapsulation of nMOFs will finally affect the properties of the constructed biosensing platforms. However, the preparation of multipurpose nMOFs with biological functions remains a major challenge.

* Corresponding author. Analytical & Testing Center, Sichuan University, Chengdu, Sichuan, 610064, China.
E-mail address: lvy@scu.edu.cn (Y. Lv).

https://doi.org/10.1016/j.talanta.2019.03.107
Received 26 January 2019; Received in revised form 25 March 2019; Accepted 30 March 2019
Available online 02 April 2019
0039-9140/

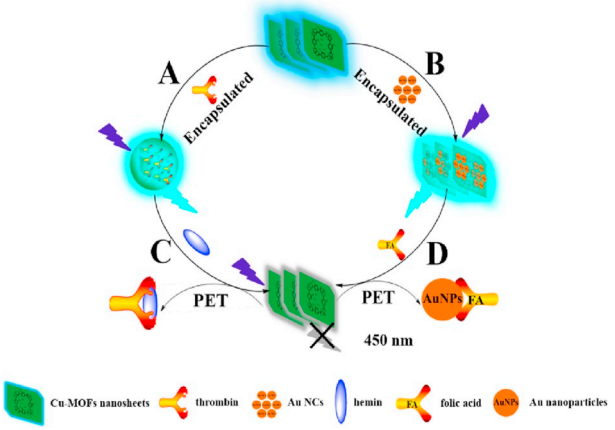

Scheme 1. A: Schematic illustration of thrombin encapsulated MOFs nanosheets process. **B:** Schematic illustration of Au NCs encapsulated MOFs nanosheets process. **C:** Schematic illustrations of the analysis of hemin using thrombin encapsulated MOFs nanocomposites. **D:** Schematic illustrations of the analysis of FA using Au-NCs encapsulated MOFs nanocomposites.

Therefore, multipurpose nMOFs are the significant strategy for the construction of functionalized MOFs and signal-transduction pathway.

Herein, multipurpose nMOFs with biological functions were realized through encapsulation of thrombin and Au NCs respectively. Simultaneously, the blue fluorescence of Cu-MOFs nanosheets was enhanced with binding thrombin or Au NCs, accompanied by greatly improved in water solubility of MOFs nanocomposites (Scheme 1A, 1B). The results indicated that the strategies of multipurpose MOFs nanocomposites were constructed. In this encapsulation process, the formed MOFs nanocomposites displayed strong fluorescence, and can be used to develop the biosensors for the recognition of target biomolecules with high selectivity and sensitivity. When hemin and folic acid (FA) was introduced to the formed MOFs nanocomposites, thrombin-hemin complex and Au nanoparticles-folic acid complex was formed respectively, photoinduced electron transfer (PET) from MOFs nanocomposites to thrombin-hemin complex or Au nanoparticles-folic acid complex was realized, and resulted in quenching fluorescence of the MOFs nanocomposites (Scheme 1C, 1D). This unique multipurpose encapsulation properties of nMOFs provided a novel concept for construction versatile fluorescence biosensors.

2. Experimental section

2.1. Synthesis of water-soluble fluorescence NH_2-Cu-MOFs nanosheets

The synthesis of MOFs nanosheets was developed from the reported reference [29,30] with modifications. Described as follows: 35 mL of deionized water dissolved with 3 mmol $Cu(NO_3)_2{\cdot}3H_2O$ and then 3 mmol NH_2-H_2BDC was added to the solution under magnetic stirring. After 30 min, appropriate amount of urea was added into the above solution, and then continuing magnetic stirring for 30 min. Then the obtained mixed solution was placed in a 50 mL Teflon-lined autoclave and maintained the temperature at 150 °C for 10 h. And then cooling it down to room temperature, the dark-green solution was obtained by centrifugation at 6000 rpm for 10 min. Then the excessive amounts of acetone was added to the supernatant and dark-green precipitates were collected by centrifugation at 10000 rpm for 15 min. The above dark-green precipitates were purified by refluxing in DMF at 120 °C for 6 h and then the resulting dark-green production was separated from the resulting solution by suction filtration and washed with excess DMF and acetone respectively. The obtained products were dried at 50 °C overnight and then collected.

2.2. Synthesis water solubility GSH-Au NCs

GSH-Au NCs were obtained according to the literature procedures with modifications [31]. The brief description is as follows: the fresh prepared GSH aqueous solutions (6 mM, 20 mL) were added into 100 mL three flask under gentle stirring at room temperature and then bubbled N_2 for about 30 min to dislodge dissolved oxygen. Then, $HAuCl_4$ (4 mM, 20 mL) were added the above solution drop by drop. The formed solution was heated to 90 °C under magnetic stirring for 24 h under the atmosphere of nitrogen. The obtained GSH-Au NCs (1×10^{-4} mol/L) were stored at 4 °C for further use.

2.3. Synthesis water solubility fluorescence MOFs-Thrombin nanocomposites and MOFs-Au NCs nanocomposites

In a typical experiment, at room temperature, a solution of MOFs nanosheets (25 μg/mL, 300 μL), 200 μL pH = 7.4 Tris-HCl, and appropriate amounts of thrombin (500 μg/mL) and GSH-Au NCs (1×10^{-4} mol/L) were added to a 2 mL reaction tube and mixed sufficiently with gentle shake respectively. And then about 30 min, MOFs-thrombin and MOFs-Au NCs nanocomposites were obtained respectively. They were quite stable at 4 °C for a month without any change and were stored in the fridge at 4 °C for further use.

2.4. Fluorescence detection of hemin and folic acid

MOFs nanosheets (25 μg/mL, 300 μL), 200 μL pH = 7.4 Tris-HCl, and thrombin (500 μg/mL, 250 μL) were added into a 2 mL colorimetric tube and mixed thoroughly with gentle shake. About 30 min later, appropriate amounts of hemin or folic acid was added into the 2 mL colorimetric tube, then diluted it with deionized water to the mark and mixed thoroughly. After incubated for 10 min, the fluorescence spectra and UV–vis spectra of the solution were measured.

2.5. Real samples detection

The potential application of the developed methods for hemin and folic acid analysis in biological media was verified, the assay of hemin and folic acid in human serum samples was performed. Different concentrations of hemin and folic acid were gain the result the human serum samples, and the results were obtained by the method of standard addition.

3. Results and discussion

3.1. Encapsulation and characterization of MOFs-thrombin nanocomposites

To demonstrate such multipurpose encapsulated MOFs nanocomposites formed process, fluorescence MOFs nanosheets were successfully synthesized with urea as the synthesis morphology modulator and the obtained MOFs nanosheets displayed water solubility in aqueous solution. Transmission electron microscopy (TEM) was utilized to characterize the MOFs nanosheets (Fig. 1A). It illustrated that MOFs nanosheets remained drastic aggregation although the concentration of MOFs nanosheets was very low (3.75 μg/mL). After thrombin was added into the MOFs nanosheets suspended liquid, MOFs-thrombin nanocomposites showed excellent water solubility and monodispersed nanosheets (Fig. 1B). The XPS (Fig. S1) revealed that the bind energy of Cu^{2+} was 932 eV and 952 eV for MOFs nanosheets, which are readily assigned to the $Cu2p_{3/2}$ and $Cu2p_{1/2}$. According to the XRD patterns (Fig. 1C) of the MOFs obtained with different concentration of urea, it can be found that MOFs nanosheets with good crystallinity can be obtained with relatively low concentration of urea. Interestingly, the formed MOFs-thrombin nanocomposites emit stronger blue fluorescence (445 nm) under the excitation of 365 nm than MOFs nanosheets (Fig. 1D). Besides, the FL intensity of MOFs-thrombin nanocomposites

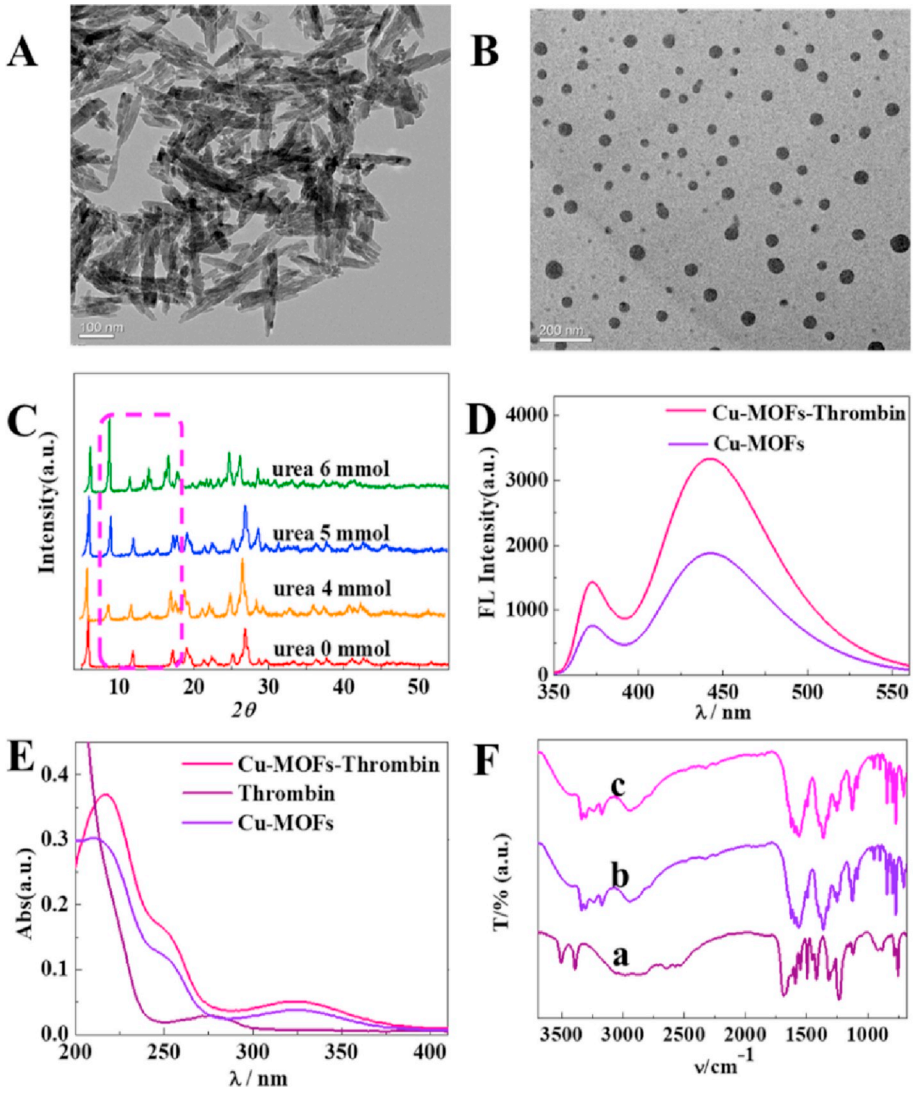

Fig. 1. A: TEM image of MOFs nanosheets **B**: TEM image of MOFs-thrombin nanocomposites. **C**: XRD spectra of MOFs nanosheets. **D**: Fluorescence emission spectra of MOFs nanosheets and MOFs-thrombin nanocomposites. The concentration of MOFs nanosheets: 3.75 μg/mL, thrombin: 62.5 μg/mL. **E**: UV–vis spectra of MOFs nanosheets, thrombin and MOFs-thrombin nanocomposites. The concentration of MOFs nanosheets: 3.75 μg/mL, thrombin: 62.5 μg/mL. **F**: FTIR spectra of materials and the system. a: FTIR spectra of NH_2-H_2BDC; b: MOFs nanosheets; c: MOFs-thrombin nanocomposites.

was enhanced with the increase of thrombin concentration (Fig. S2). UV–vis spectra response of MOFs nanosheets upon addition of thrombin before and after were studied and shown in Fig. 1E. From UV–vis spectra, it displayed that characteristic absorption peak (275 nm) of thrombin disappeared simultaneously produced a new absorption peak (223 nm). It was illustrated that the MOFs-thrombin nanocomposites were formed successfully. Furthermore, FTIR spectra of the MOFs nanosheets and MOFs-thrombin nanocomposites were shown in Fig. 1F. From the FTIR spectra, it can be seen that N-H (1147 cm^{-1}) and C═O (1685 cm^{-1}) stretching band of MOFs-thrombin nanocomposites get weaker, identifying the successful encapsulation of thrombin on the surface of MOFs nanosheets through hydrogen bond. The reason for the fluorescence enhancement of MOFs nanosheets in this system may be the formation of a conjugate junction between MOFs nanosheets and thrombin, thus causing reduction of surface defects on MOFs nanosheets. The UV–vis absorption of the MOFs-thrombin nanocomposites was greatly higher with the presence of thrombin (Fig. 1E), which indicated that the enhancement fluorescence intensity may be induced by the increase in the excitation wavelength [32]. These results indicated that functionalization of thrombin onto MOFs nanosheets could effectively reduce its surface defects, thereby enhancing the fluorescence emission (Scheme 1A).

3.2. Construction of fluorescence biosensor

Considering the strong fluorescence of MOFs-thrombin nanocomposites, we aim to utilize this novel system to develop a new sensing platform for specific determination. Hemin, as powerful electron receptor, was found to have a strong quenching effect on fluorescence of MOFs-thrombin nanocomposites, offering a possibility for its analysis, as depicted schematically in Scheme 1C. To obtain optimal sensing performance of the proposed chemical probe, experimental conditions were systematically investigated (Fig. 2). Firstly, the thrombin concentration response to the fluorescence intensity of MOFs was investigated. In Fig. 2A, the fluorescence intensity of MOFs-thrombin nanocomposites stably enhanced about double than the original MOFs nanosheets when 62.5 μg/mL of thrombin was incorporated into 300 μL MOFs nanosheets (25 μg/mL) suspended liquid. Therefore, the concentration of thrombin 62.5 μg/mL was chosen for the further experiment. The effect of functionalized reaction time between MOFs nanosheets and thrombin in solution was shown in Fig. 2B. The FL intensity enhanced with the increasing of reaction time and then

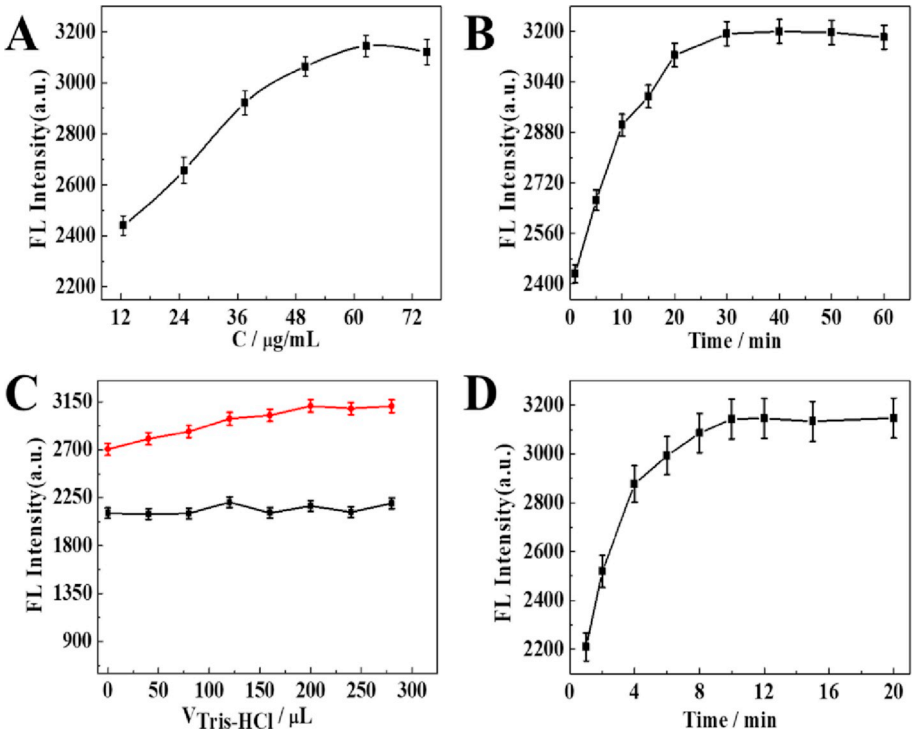

Fig. 2. A: The effect of thrombin concentration on MOFs nanosheets fluorescence intensity. MOFs nanosheets: 3.75 μg/mL, Tris-HCl, pH = 7.4, 200 μL. **B:** The effect of incubation time on MOFs nanosheets-thrombin nanocomposites fluorescence intensity. MOFs nanosheets: 3.75 μg/mL, thrombin: 62.5 μg/mL, Tris-HCl, pH = 7.4, 200 μL. **C:** The effect amount of Tris-HCl on MOFs nanosheets-thrombin nanocomposites-hemin fluorescence intensity. MOFs nanosheets: 3.75 μg/mL, thrombin: 62.5 μg/mL, Tris-HCl, pH = 7.4. **D:** The time dependent fluorescence intensity of the system after addition of hemin. MOFs nanosheets: 3.75 μg/mL, thrombin: 62.5 μg/mL, hemin 12.5 μg/mL, Tris-HCl, pH = 7.4, 200 μL.

reached a relatively stable value after 30 min, so the suitable time was 30 min for the combination MOFs nanosheets with thrombin. The effect of the buffer solutions, such as sodium acetic acid-sodium acetate, Tris-HCl and PBS buffer solutions on the fluorescence intensities of the system was discussed. The results illustrated that Tris-HCl was the optimal buffer solution for the system. The pH range of the system is an important relevant to MOFs-thrombin nanocomposites formation and the fluorescence detection of hemin. Considering the probable application in real samples, pH 7.4 Tris-HCl was chosen as the optimal pH value for the further experiments. According to the results shown in Fig. 2C and 200 μL of Tris-HCl buffer solution of pH = 7.4 was then chosen for the reaction. The incubation time of MOFs-thrombin nanocomposites combination with hemin was discussed. After the incubation time for 10 min, the fluorescence intensity signal increased and approached a stable platform (Fig. 2D). Consideration of the sensitivity and time efficiency of the system, 10 min was chosen for further experiments.

3.3. Mechanism of the fluorescence sensing

To explore the mechanism of the fluorescence quenching of MOFs-thrombin nanocomposites by hemin, the TEM observations (Fig. 3A) confirmed the dissociation of MOFs-thrombin nanocomposites and the formation of thrombin-hemin complex. Besides, the corresponding SEM images (Fig. S3) were obtained. From the SEM images, the structure and morphology of MOFs-thrombin nanocomposites changed from monodispersed spherical particles to cubic aggregation and thrombin-hemin aggregation. We know that thrombin was immobilized onto MOFs nanosheets surfaces through hydrogen bonding or electrostatic attraction between $-NH_2$ of MOFs nanosheets and $-COO^-$ of thrombin. So we speculated that hemin could compete to bind with thrombin through intermolecular hydrogen bonding interaction, leading to disintegration of MOFs-thrombin nanocomposites and resulting in cubic aggregation of nMOFs. To confirm the speculation, UV–vis absorption spectra of thrombin, hemin and thrombin-hemin complex were obtained and shown in Fig. 3B. It can be seen that the slight blue shift absorption peak is assigned to the $n-\pi^*$ transition of the C═O band at about 325 nm [33], which indicated that hemin may react with thrombin and form thrombin-hemin complex. As further evidences for the formation of thrombin-hemin complex, FTIR spectra of hemin (-C═O, 1700 cm^{-1}) changed obviously and was shown in Fig. 3C. It indicated that hydrogen bonds may play a key role in the interaction between thrombin and hemin.

As we all know, hemin has powerful electron receptor effect and can accept the excited state electron [34]. In this case, we studied the interaction between MOFs nanosheets and hemin to further explain the fluorescence quench mechanisms. From Fig. S4, it can be seen that the fluorescence of MOFs nanosheets was quenched by hemin with a series of different concentrations, which indicated that hemin was a crucial factor in quenching FL of MOFs nanosheets. Therefore, we deduced that excited state electron of MOFs-thrombin nanocomposites was captured by hemin when MOFs-thrombin nanocomposites were excited by UV light (365 nm), which induced the electron-hole of MOFs-thrombin nanocomposites cannot be combined and FL of MOFs-thrombin nanocomposites was quenched by hemin. To verify the process of FL quenching, time-resolved fluorescence decay spectra (Fig. 3D) in the absence and presence of hemin were obtained and it indicated that the fluorescence lifetime of MOFs-thrombin nanocomposites unchanged after addition hemin, which illustrated that the fluorescence quenching of MOFs-thrombin nanocomposites triggered by hemin may be dominantly due to static quenching effect rather than dynamic quenching effect [35]. Therefore, photoinduced electron transfer and the cubic aggregation of nMOFs might synergistically induce to FL quenching of MOFs-thrombin nanocomposites.

3.4. Sensitivity and selectivity

Under the optimum experimental conditions, applicability of the sensing system for quantitatively detection of hemin was evaluated. As shown in Fig. 4A, the fluorescence of the MOFs-thrombin nanocomposites was quenched obviously with increasing the concentration of hemin with a wide response range (0.16 μg/mL-12.5 μg/mL) and a very low detection limit (0.047 μg/mL, 3σ/K) with a regression coefficient of 0.9932. The linear regression equation is $I = 172.44C + 166.08$ (where C is the concentration of hemin, μg/mL). The relative standard deviation (RSD) for eleven replicate detection is

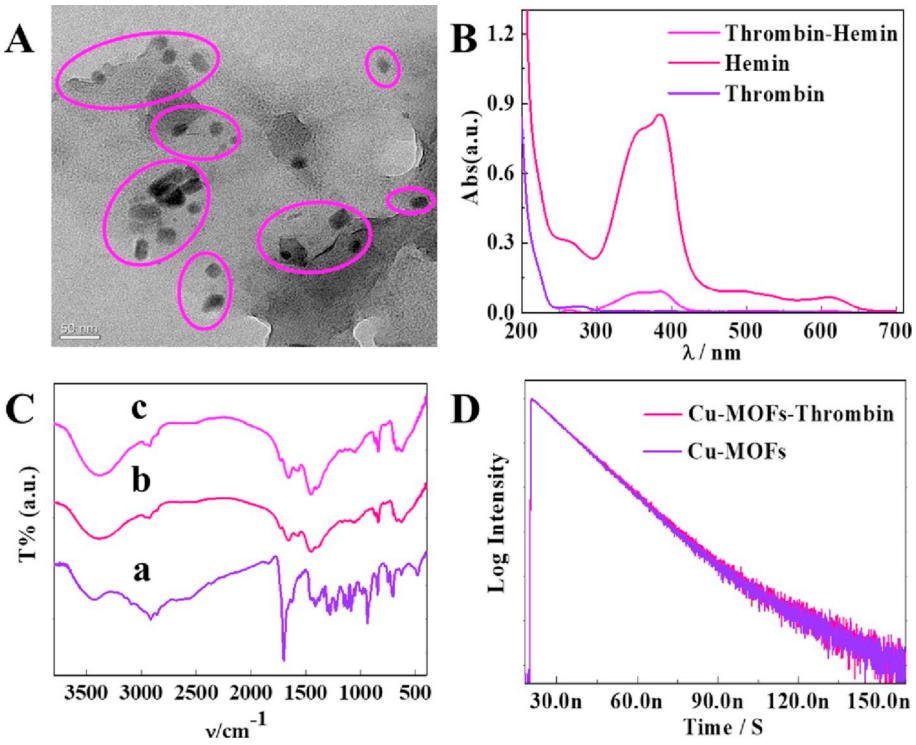

Fig. 3. A: TEM image of MOFs-thrombin nanocomposites-hemin complex. **B:** UV–vis spectra of hemin, thrombin and thrombin-hemin complex. The concentration of MOFs nanosheets: 3.75 μg/mL, thrombin: 62.5 μg/mL, hemin: 12.5 μg/mL. **C:** FTIR spectra of materials and the products. a: FTIR spectra of hemin; b: MOFs nanosheets-thrombin nanocomposites; c: hemin-thrombin complex. **D:** Time-resolved fluorescence decay spectra of thrombin functionalized MOFs nanosheets and MOFs nanosheets-thrombin nanocomposites-hemin complex.

2.7%. It indicates that the developed strategy is sensitivity and will be a valuable strategy for detection hemin.

To evaluate the stability of the developed strategy, the high selectivity is important in real sample detection. Therefore, the selectivity of the MOFs-thrombin nanocomposites fluorescence sensing system was estimated and shown in Fig. 4B. Besides, the effects of five other kinds of enzyme and protein, including lysozyme, trypsin, papain, BSA and HSA at the same concentration of hemin, on the fluorescence response of MOFs-thrombin nanocomposites containing 12.5 μg/mL hemin were investigated simultaneously. From the experimental results, it can be found that the fluorescence intensity of MOFs-thrombin nanocomposites was significantly quenched by hemin, however, almost no effect of the fluorescence intensity was observed in the presence of other enzyme and protein. Considering the complex components of the human serum samples, the selectivity of the MOFs-thrombin nanocomposites-based biosensor for hemin over some commonly existing cation, anions and amino acid including Na^+, K^+, Ca^{2+}, Mg^{2+}, Cl^-, NO_3^-, SO_4^{2-}, glycine, tryptophan, valine, leucine, phenylalanine, proline, serine, asparagine, lysine, arginine, glutamic acid were considered. The experimental results indicated that common cation, anions and amino acids have no effect on the biosensor performance. Obviously, the results indicated that the MOFs-thrombin nanocomposites biosensing system exhibits high selectivity for hemin.

3.5. Application in human serum samples

The potential application of the MOFs-thrombin nanocomposites to detection of hemin in human serum samples was verified. Volunteers (Sichuan university Hospital, Chengdu, China) supplied human serum samples. The International Ethical Guidelines for Biomedical Research Involving Human Subjects were conformed in all experimental procedures, and protocols were approved by Medical ethics committee of Sichuan University. 200 μL of human serum samples was added into a 2 mL reaction tube. Following the experimental procedure, RSD and recovery were examined by using the method of standard addition. The results were displayed in Table S1. The recoveries for samples detection were in the range of 97%–101%. The results indicated that the developed strategy was suitable for hemin assay in human serum samples with high reliability and accuracy.

3.6. Universality of the strategy

The universality of present proof-of-concept was demonstrated by a homogeneous model, which was implemented for detection of folic acid. As shown in Scheme 1B, Au NCs adsorbed on the surface of the MOFs nanosheets through electrostatic attraction, and self-assembly of the MOFs-Au NCs nanocomposites. After the FA introduced, Au NCs

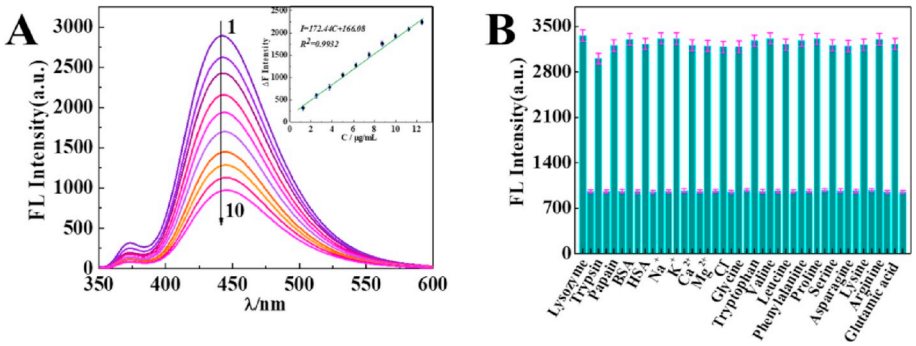

Fig. 4. A: Fluorescence spectra and validation (insert) of the use of MOFs-thrombin nanocomposites as probe for detection of hemin. MOFs-thrombin nanocomposites: MOFs nanosheets 3.75 μg/mL, thrombin 62.5 μg/mL, Tris-HCl, pH = 7.4, 200 μL. **B:** Selectivity of the MOFs-thrombin nanocomposites biosensor for hem in presence of interference. The concentration of them is 12.5 μg/mL, respectively.

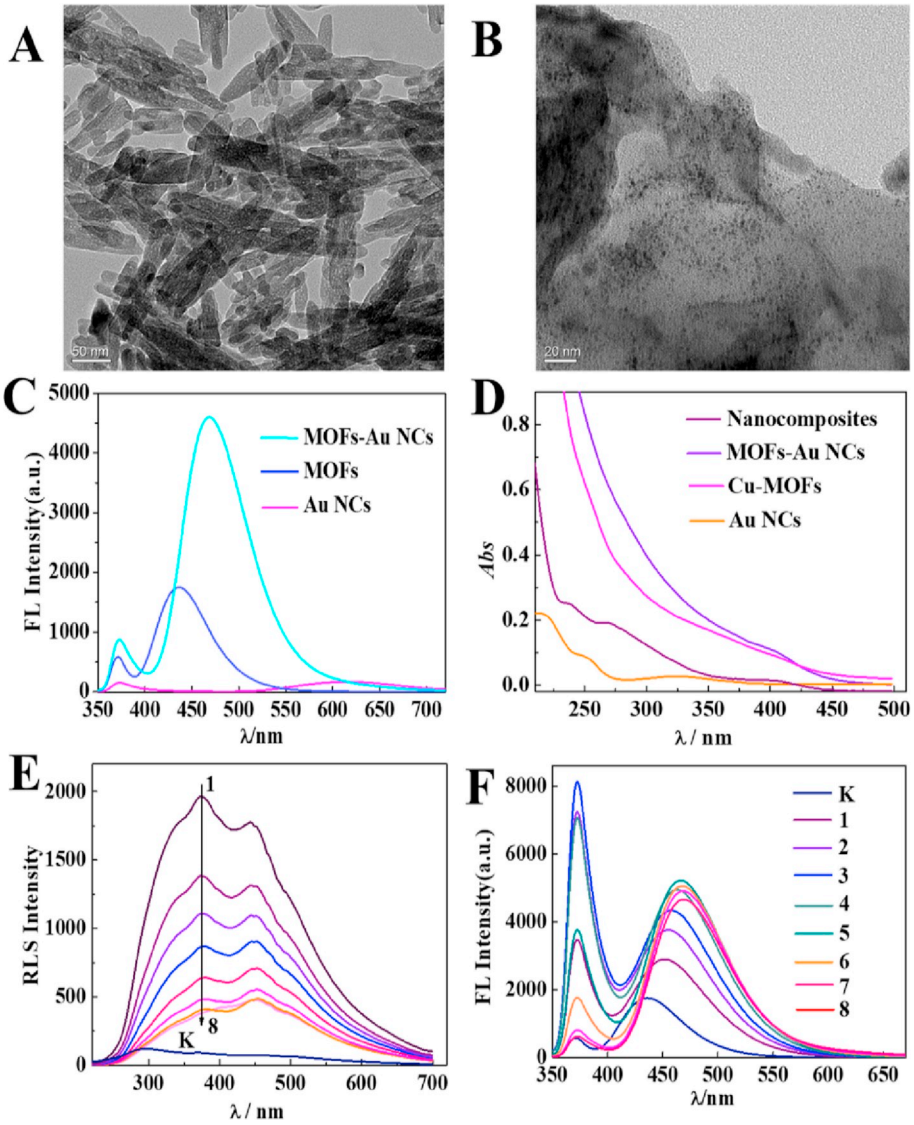

Fig. 5. A: TEM image of MOFs nanosheets. **B:** TEM image MOFs-Au NCs nanocomposites. **C:** Fluorescence emission spectra of Au NCs, MOFs nanosheets and MOFs-Au NCs nanocomposites. Au NCs: 5 μmol/L, MOFs nanosheets, 3.75 μmol/L. **D:** UV–vis spectra of the materials. a: Au NCs, b: MOFs nanosheets, c: MOFs-Au NCs nanocomposites. d: MOFs-Au NCs nanocomposites (MOFs nanosheets as reference). RLS spectra **(E)** and Fluorescence spectra (**F**) of MOFs nanosheets in the presence of different concentration of Au NCs. K: MOFs nanosheets. The concentration of MOFs nanosheets: 3.75 μmol/L. 1–8: Au NCs: 0.25, 0.5, 0.75, 1, 2, 4, 6, 8 μmol/L.

competed to bind with FA to form Au NCs-FA complex, thus leading to quenching of fluorescence of the MOFs-Au NCs nanocomposites (Scheme 1D). From the results shown in Fig. 5, it could be seen that TEM was utilized to characterize the MOFs nanosheets (Fig. 5A). It illustrated that MOFs nanosheets remained drastic aggregation. After Au NCs was added into the MOFs nanosheets suspended liquid, MOFs-Au NCs nanocomposites were formed (Fig. 5B). Meanwhile, fluorescence of Au NCs declined while that of MOFs-Au NCs nanocomposites increased (Fig. 5C) when Au NCs adsorbed on surface of MOFs nanosheets, illustrating the formation of MOFs-Au NCs nanocomposites. It was further confirmed by UV–vis spectra deriving from the interaction between Au NCs and MOFs nanosheets (Fig. 5D), where an apparently new absorption peak at 275 nm appeared. Interestingly, the resonance light scattering intensity of the MOFs nanosheets gradually decreased (Fig. 5E) and the fluorescence intensity of the MOFs-Au NCs nanocomposites increased (Fig. 5F) with the presence of Au NCs of increasing concentrations. We concluded that the water solubility of the MOFs-Au NCs nanocomposites improved obviously [36], and it may be the reason of fluorescence enhancement of MOFs-Au NCs nanocomposites.

We further researched the impact of FA on MOFs-Au NCs nanocomposites by means of TEM and UV–vis absorption spectroscopy. According to TEM images in Fig. 6A, we speculated that FA could bind with Au NCs, which induced desorption of Au NCs from the MOFs-Au NCs nanocomposites surface and aggregated to form Au nanoparticles (Au NPs) and finally self-assembled Au NPs-FA complex. The UV–vis spectra results (Fig. 6B) showed that there were two peaks at 280 nm and 350 nm for FA, while intensity of the absorption peak at 280 nm was weakened after interaction with MOFs-Au NCs nanocomposites. As energy receptor and photoelectron acceptor, lead to quenching of the fluorescence of the MOFs-Au NCs nanocomposites.

Under the optimum experimental conditions (Fig. S5), fluorescence spectra of the MOFs-Au NCs nanocomposites after addition to different concentrations of FA were measured. Fig. 6C showed the relationship between the quenched fluorescence of the MOFs-Au NCs nanocomposites and the FA concentration, and the inset showed the related calibration curve. The results illustrated the linear range of 0.153–17.5 μmol/L and LOD of 45 nmol/L (3σ/K) for FA, which is much lower than the average FA level in human serum. Therefore, the developed method is expected to be used for FA detection in human serum

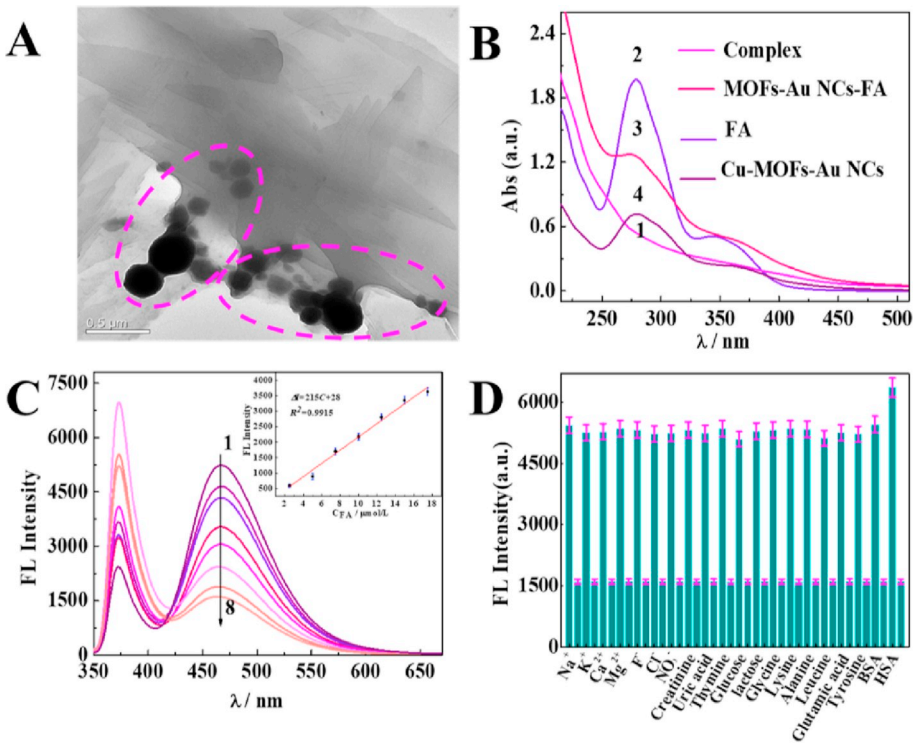

Fig. 6. A: TEM image of MOFs-Au NCs nanocomposites-FA. **B:** UV-vis spectra of the interaction between MOFs-Au NCs nanocomposites and FA. a: MOFs-Au NCs nanocomposites. b: FA. c: MOFs-Au NCs nanocomposites-FA. d: MOFs-Au NCs nanocomposites-FA (MOFs-Au NCs nanocomposites as reference). **C:** Fluorescence spectra and validation (insert) of the use of MOFs-Au NCs nanocomposites as probe for detection of FA. MOFs nanosheets 3.75 μg/mL, Au NCs: 5 μmol/L, Tris-HCl, pH = 7.4, 150 μL. **D:** Selectivity of the MOFs-Au NCs nanocomposites biosensor for FA in presence of interference. The concentration of them is 17.5 μmol/L, respectively.

samples. Subsequently, we tested interferences of various cations, anions and biomolecules commonly existed in human serum samples on the proposed sensing system so as to evaluate its feasibility. From the results in Fig. 6D, it was found that apart from FA, all the tested substances nearly had no quenching effect on fluorescence of MOFs-Au NCs nanocomposites, illustrating the high selectivity of this strategy for FA detection. Based on the excellent analytical performance of the proposed method, the application of MOFs-Au NCs nanocomposites as a fluorescence probe for detecting FA in human serum was carried out. The recoveries for samples detection via standard addition method were in the range of 98%–103% and the relative standard deviation was 3.3% (Table S2). This method exhibits outstanding in a range and satisfactory selectivity and successfully applied to FA detection in serum. The comparison between the properties of merit of MOFs-Au NCs nanocomposites probe with the previously reported (Table S3). It illustrated that the biosensor may be categorized among the good FA probe ever reported. All the results show that the MOFs-Au NCs nanocomposites has a good application prospects in the construction of biosensors.

4. Conclusions

This work achieved that the strategies can be apply to multiple targets with only modulating encapsulant. The introduction of multiple encapsulant triggered the binding with targets and subsequent formation of specific binding complex. This work designs a new system involving enhancement nMOFs fluorescence through formation of MOFs nanocomposites that can be utilized to improve the sensitivity and selectivity of fluorescence biosensors for detection hemin and FA. Compared to the traditional MOFs, encapsulated enhancement water solubility fluorescence nMOFs show the specific and excellent application prospect. The strategies avoids complex labeling processes and do not require troublesome procedures. The MOFs-thrombin nanocomposites and MOFs-Au NCs nanocomposites were obtained via one-pot encapsulation of MOFs nanosheets with thrombin and Au NCs respectively, which showed better water solubility and higher fluorescence properties. This research also provided a successful strategic thought for exploring new and interesting properties of functionalized nMOFs and extending their applications in analytical chemistry.

Acknowledgments

The authors gratefully acknowledge financial support from the National Natural Science Foundation of China (Grants 21575093 and 21505095). This work is also supported by the Science and Technology Department of Sichuan Province(19YYJC2423) and the Fundamental Research Funds for the Central Universities. Prof. Yingying Su from Analytical & Testing Center of Sichuan University is gratefully thanked for technical assistance.

Appendix A. Supplementary data

Supplementary data to this article can be found online at https://doi.org/10.1016/j.talanta.2019.03.107.

References

[1] W. Ma, Q. Jiang, P. Yu, L. Yang, L. Mao, Zeolitic imidazolate framework-based electrochemical biosensor for in vivo electrochemical measurements, Anal. Chem. 85 (2013) 7550–7557.
[2] D. Wang, M. Wang, Z. Li, Fe-based metal-organic frameworks for highly selective photocatalytic benzene hydroxylation to phenol, ACS Catal. 5 (2015) 6852–6857.
[3] D. Kukkar, K. Vellingiri, K.H. Kim, A. Deep, Recent progress in biological and chemical sensing by luminescent metal-organic frameworks, Sensor. Actuator. B Chem. 273 (2018) 1346–1370.
[4] C. Cui, Q. Wang, Q. Liu, X. Deng, T. Liu, D. Li, X. Zhan, Porphyrin-based porous organic framework: an efficient and stable peroxidase-mimicking nanozyme for detection of H_2O_2 and evaluation of antioxidant, Sensor. Actuator. B Chem. 277 (2018) 86–94.
[5] P. Ling, J. Lei, L. Zhang, H. Ju, Porphyrin-encapsulated metal-organic frameworks as mimetic catalysts for electrochemical DNA sensing via allosteric switch of hairpin DNA, Anal. Chem. 87 (2015) 3957–3963.
[6] Q.S. Wang, J.J. Li, M.N. Zhang, X. Li, A luminescent Eu(III)-based metal-organic framework as a highly effective sensor for cation and anion detections, Sensor. Actuator. B Chem. 258 (2018) 358–364.
[7] Y. Zhang, S. Yuan, G. Day, X. Wang, X. Yang, H.C. Zhou, Luminescent sensors based on metal-organic frameworks, Coord. Chem. Rev. 354 (2018) 28–45.
[8] J.M. Pietryga, Y.S. Park, J. Lim, A.F. Fidler, W.K. Bae, S. Brovelli, V.I. Klimov, Spectroscopic and device aspects of nanocrystal quantum dots, Chem. Rev. 116

(2016) 10513–10622.
[9] L. Qin, L.X. Lin, Z.P. Fang, S.P. Yang, G.H. Qiu, J.X. Chen, W.H. Chen, A water-stable metal-organic framework of a zwitterionic carboxylate with dysprosium: a sensing platform for Ebolavirus RNA sequences, Chem. Commun. 52 (2016) 132–135.
[10] H.S. Wang, H.L. Liu, K. Wang, Y. Ding, J.J. Xu, X.H. Xia, H.Y. Chen, Insight into the unique fluorescence quenching property of metal-organic frameworks upon DNA binding, Anal. Chem. 89 (2017) 11366–11371.
[11] S. Patra, T.H. Crespo, A. Permyakova, C. Sicard, C. Serre, A. Chaussé, N. Steunou, L. Legrand, Design of metal organic framework-enzyme based bioelectrodes as a novel and highly sensitive biosensing platform, J. Mater. Chem. B 3 (2015) 8983–8992.
[12] S. Hu, J. Yan, X. Huang, L. Guo, Z. Lin, F. Luo, B. Qiu, K.Y. Wong, G. Chen, A sensing platform for hypoxanthine detection based on amino-functionalized metal organic framework nanosheet with peroxidase mimic and fluorescence properties, Sensor. Actuator. B Chem. 267 (2018) 312–319.
[13] X. Lian, Y. Fang, E. Joseph, Q. Wang, J. Li, S. Banerjee, C. Lollar, X. Wang, H.C. Zhou, Enzyme-MOFs (metal-organic framework) composites, Chem. Soc. Rev. 46 (2017) 3386–3401.
[14] S.S. Nagarkar, T. Saha, A.V. Desai, P. Talukdar, S.K. Ghosh, Metal-organic framework based highly selective fluorescence turn-on probe for hydrogen sulphide, Sci. Rep. 4 (2014) 7053.
[15] V.M. Suresh, S.J. George, T.K. Maji, MOF nano-vesicles and toroids: self-assembled porous soft-hybrids for light harvesting, Adv. Funct. Mater. 23 (2013) 5585–5590.
[16] T. Lu, L. Zhang, M. Sun, D. Deng, Y. Su, Y. Lv, Amino-functionalized metal-organic frameworks nanoplates-based energy transfer probe for highly selective fluorescence detection of free chlorine, Anal. Chem. 88 (2016) 3413–3420.
[17] A. Monguzzi, M. Ballabio, N. Yanai, N. Kimizuka, D. Fazzi, M. Campione, F. Meinardi, Highly fluorescent metal-organic-framework nanocomposites for photonic applications, Nano Lett. 18 (2018) 528–534.
[18] H.S. Wang, W.J. Bao, S.B. Ren, M. Chen, K. Wang, X.H. Xia, Fluorescent sulfur-tagged europium(III) coordination polymers for monitoring reactive oxygen species, Anal. Chem. 87 (2015) 6828–6833.
[19] T. Xia, T. Song, Y. Cui, Y. Yang, G. Qian, A dye encapsulated terbium-based metal-organic framework for ratiometric temperature sensing, Dalton Trans. 45 (2016) 18689–18695.
[20] Y. Cui, Y. Yue, G. Qian, B. Chen, Luminescent functional metal-organic frameworks, Chem. Rev. 112 (2012) 1126–1162.
[21] J. Pang, Y. Liao, X. Huang, Z. Ye, D. Yuan, Metal-organic framework-monolith composite-based in-tube solid phase microextraction on-line coupled to high-performance liquid chromatography-fluorescence detection for the highly sensitive monitoring of fluoroquinolones in water and food samples, Talanta 199 (2019) 499–506.
[22] Y. Zhang, B. Yan, A ratiometric fluorescent sensor with dual response of Fe^{3+}/Cu^{2+} based on europium post-modified sulfone-metal-organic frameworks and its logical application, Talanta 197 (2019) 291–298.
[23] C. Liu, B. Yan, A novel photofunctional hybrid material of pyrene functionalized metal-organic framework with conformation change for fluorescence sensing of Cu^{2+}, Sensor. Actuator. B Chem. 235 (2016) 541–546.
[24] J.S. Kahn, L. Freage, N. Enkin, M.A.A. Garcia, I. Willner, Stimuli-responsive DNA-functionalized metal-organic frameworks (MOFs), Adv. Mater. 29 (2017) 1602782.
[25] F. Lyu, Y. Zhang, R.N. Zare, J. Ge, Z. Li, One-pot synthesis of protein-embedded metal-organic frameworks with enhanced biological activities, Nano Lett. 14 (2014) 5761–5765.
[26] X. Lian, Y. Fang, E. Joseph, Q. Wang, J. Li, S. Banerjee, C. Lollar, X. Wang, H.C. Zhou, Enzyme-MOFs (metal-organic framework) composites, Chem. Soc. Rev. 46 (2017) 3386–3401.
[27] F. Moro, L. Turyanska, J. Wilman, H.E.L. Williams, A.J. Fielding, A. Patanè, Surface sensing of quantum dots by electron spins, Nano Lett. 16 (2016) 6343–6348.
[28] H. Weng, B. Yan, A flexible Tb(III) functionalized cadmium metal organic framework as fluorescent probe for highly selectively sensing ions and organic small molecules, Sensor. Actuator. B Chem. 228 (2016) 702–708.
[29] J.M. Chin, E.Y. Chen, A.G. Menon, H.Y. Tan, A.T.S. Hor, M.K. Schreyer, J. Xu, Tuning the aspect ratio of NH_2-MIL-53(Al) microneedles and nanorods via coordination modulation, CrystEngComm 15 (2013) 654–657.
[30] T. Ahnfeldt, D. Gunzelmann, T. Loiseau, D. Hirsemann, J. Senker, G. Ferey, N.-Stock, Synthesis and modification of a functionalized 3D open-framework structure with MIL-53 topology, Inorg. Chem. 48 (2009) 3057–3064.
[31] L. J Zhang, N. He, C. Lu, Aggregation-induced emission: a simple strategy to improve chemiluminescence resonance energy transfer, Anal. Chem. 87 (2015) 1351–1357.
[32] H. Aouani, J. Wenger, D. Gérard, H. Rigneault, E. Devaux, T.W. Ebbesen, F. Mahdavi, T. Xu, S. Blair, Crucial role of the adhesion layer on the plasmonic fluorescence enhancement, ACS Nano 3 (2009) 2043–2048.
[33] W.Y. Zhai, C.X. Wang, P. Yu, Y.X. Wang, L.Q. Mao, Single-layer MnO_2 nanosheets suppressed fluorescence of 7-hydroxycoumarin: mechanistic study and application for sensitive sensing of ascorbic acid in vivo, Anal. Chem. 86 (2014) 12206–12213.
[34] Y. Zang, J. Lei, L. Zhang, H. Ju, In situ generation of electron acceptor for photoelectrochemical biosensing via hemin-mediated catalytic reaction, Anal. Chem. 86 (2014) 12362–12368.
[35] S. Jin, H.J. Son, O.K. Farha, G.P. Wiederrecht, J.T. Hupp, Energy transfer from quantum dots to metal-organic frameworks for enhanced light harvesting, J. Am. Chem. Soc. 135 (2013) 955–958.
[36] J.N. Tisserant, R. Bronnimann, R. Hany, S. Jenatsch, F.A. Nuesch, R. Mezzenga, G.L. Bona, J. Heier, Resonance light scattering in dye-aggregates forming in dewetting droplets, ACS Nano 8 (2014) 10057–10065.